Polymeric Colorants: Statistical Copolymers of Indigo Building Blocks with Defined Structures

by **Gundula Voss***[a]), **Markus Drechsler**[b]), **Steffen Eller**[a]), **Michael Gradzielski**[c]), **Daniel Gunzelmann**[d]), **Svastik Mondal**[e]), **Sander van Smaalen**[e]), and **Claus S. Voertler**[f])

[a]) Department of Bioorganic Chemistry, University of Bayreuth, Universitaetsstrasse 30, NW I, D-95447 Bayreuth (fax: +49-921-555365; e-mail: Gundula.Voss@uni-bayreuth.de)

[b]) Department of Macromolecular Chemistry II, University of Bayreuth, D-95440 Bayreuth

[c]) Stranski-Laboratory of Physical and Theoretical Chemistry, Technical University of Berlin, D-10623 Berlin

[d]) Department of Inorganic Chemistry I, University of Bayreuth, D-95440 Bayreuth

[e]) Department of Crystallography, University of Bayreuth, D-95440 Bayreuth

[f]) Department of Biochemistry, University of Bayreuth, D-95440 Bayreuth

Dedicated to the memory of Prof. Dr. *Heinrich Zollinger* (1919–2005)

Statistical copolymers of indigo (**1a**) and *N*-acetylindigo (**1b**) building blocks with defined structures were studied. They belong to the class of polymeric colorants. The polymers consist of 5,5′-connected indigo units with keto structure and *N*-acetylindigo units with uncommon tautomeric indoxyl/indolone (=1*H*-indol-3-ol/3*H*-indol-3-one) structure (see **2a** and **2b** in *Fig. 1*). They formed amorphous salts of elongated monomer lengths as compared to monomeric indigo. The polymers were studied by various spectroscopic and physico-chemical methods in solid state and in solution. As shown by small-angle-neutron scattering (SANS) and transmission-electron microscopy (TEM), disk-like polymeric aggregates were present in concentrated solutions (DMSO and aq. NaOH soln.). Their thickness and radii were determined to be *ca.* 0.4 and *ca.* 80 nm, respectively. From the disk volumes and by a *Guinier* analysis, the molecular masses of the aggregates were calculated, which were in good agreement with each other. Defined structural changes of the polymer chains were observed during several-weeks storage in concentrated DMSO solutions. The original keto structure of the unsubstituted indigo building blocks reverted to the more flexible indoxyl/indolone structure. The new polymers were simultaneously stabilized by intermolecular H-bonds to give aggregates, preferentially dimers. Both aggregation and tautomerization were reversible upon dissolution. The polymers were synthesized by repeated oxidative coupling of 1,1′-diacetyl-3,3′-dihydroxybis-indoles **5** (from 1,1′-diacetyl-3,3′-bis(acetyloxy)bis-indoles **6**) followed by gradual hydrolysis of the primarily formed poly(*N*,*N*′-diacetylindigos) **7** (*Scheme*). *N*,*N*′-Diacetylbis-anthranilic acids **9** were isolated as by-products.

1. Introduction. – The industrial production of synthetic indigo (=2-(1,3-dihydro-3-oxo-2*H*-indol-2-ylidene)-1,2-dihydro-3*H*-indol-3-one; **1a**) started around 1900. At that time, the first high-molecular-mass compounds composed of repeating indigo units were reported [1] and patented as vat dyes [2]. The structures suggested at that time seem to be strange for the contemporary chemists because the nature of polymers as covalently connected, repeating monomer units was not yet known [3]. In the second half of the 20th century, polymeric indigo dyes **I** (*Fig. 1,a*) were used for the localization of hydrolytic enzyme activity [4a], and their application for protecting fibers against

© 2009 Verlag Helvetica Chimica Acta AG, Zürich

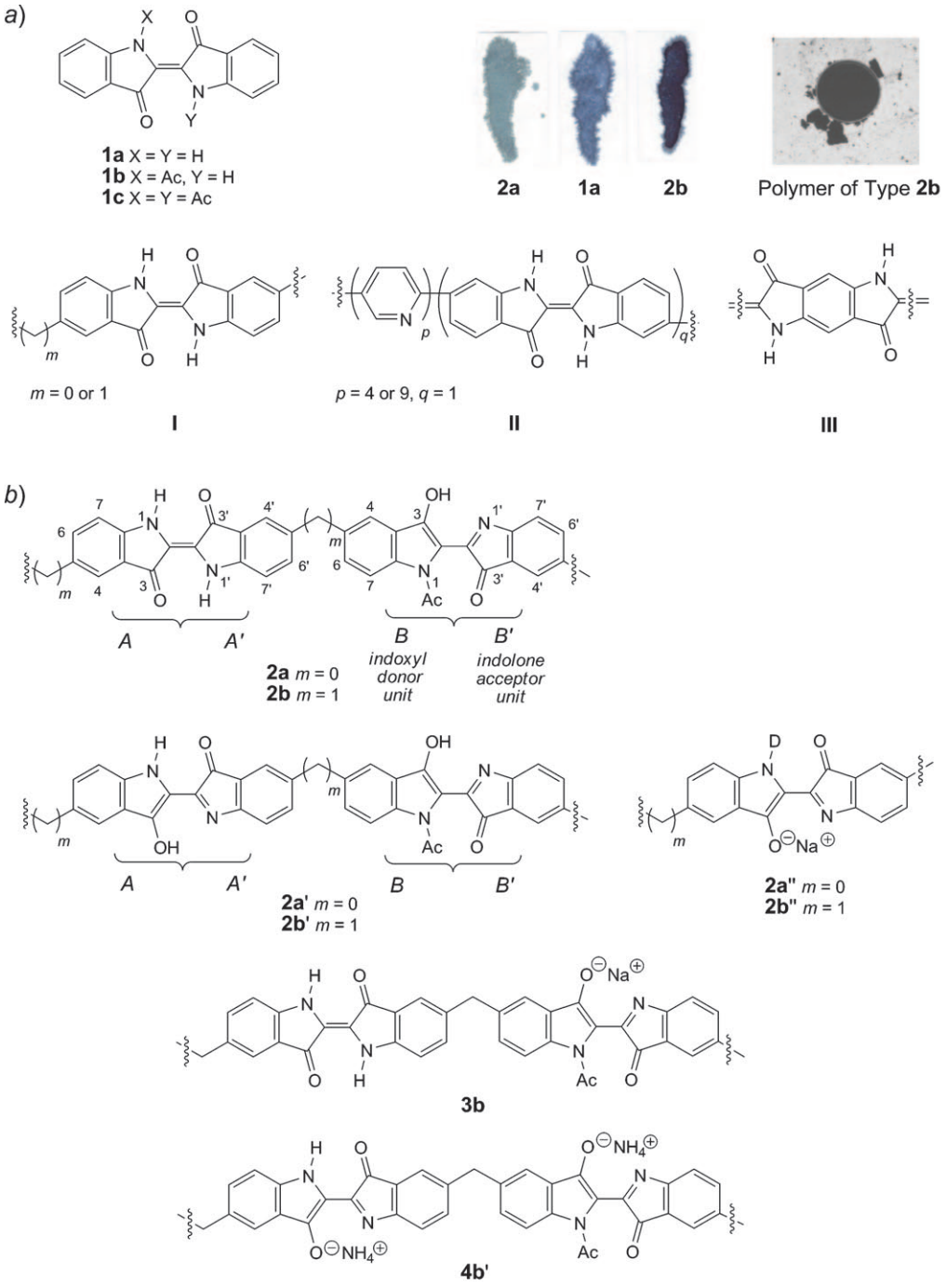

Fig. 1. a) *Indigo* (**1a**), N-*acetylindigo* (**1b**), *and* N,N′-*diacetylindigo* (**1c**), *and previously reported indigo polymers* **I** [4–6], **II** [7], *and* **III** [5a][9]. *Colored spots of reoxidized* leuco *forms of indigo* (**1a**) *and of polymers* **2a** *and* **2b** *on filter paper, and photograph of a polymer sample of type* **2b** *attracted toward a permanent magnet* (∅5.5 mm). b) *Statistical copolymers* **2a** *and* **2b** (amorphous hydrates), *polymers* **2a′** *and* **2b′** (aggregates in (D_6)DMSO, preferentially dimers), *salts* **3b** *and* **4b′** (amorphous hydrates), *and deacetylated polyanions of* **2a″** *and* **2b″** (in 0.1M NaOD)

degradation was proposed [4b]. Indigo polymers **I** were investigated as functional dyes due to semiconductive [5a–e] and ferromagnetic [6] properties. Copolymers **II** with pyridine units [7] were published. Recently, indigo polymers were reported as electrode-active masses for electrochemical equipments [8], and highly conjugated polymers **III** incorporating the bond system of indigo were patented for the production of heat- and solvent-resistant fibers and films [9].

Due to incomplete reaction and poor solubility, the purification and characterization of indigo polymers were difficult [5a,f][6]. Therefore, the objective of the presented investigations was the reproducible preparation of defined, homogeneous polymers consisting of indigo units, and the elucidation of their structures and properties, both in solid state and in solutions. Specifically, questions did arise as to: *1*) do indigo polymers form intermolecular association, and if so, *2*) what are the nature and consequences of these associations?

We present a method to obtain well-defined and homogeneous copolymers **2a** and **2b**. They consist of 5,5′-connected[1]) indigo (**1a**) and *N*-acetylindigo (**1b**) building blocks and fall into the broader class of polymeric colorants [10]. They exhibit building blocks with keto structure and with the uncommon tautomeric indoxyl/indolon structure (indoxyl = 1*H*-indol-3-ol, indolone = 3*H*-indol-3-one). The polymers were studied by means of various spectroscopic and physicochemical methods in solid state and in solution including nuclear magnetic resonance (NMR). Their sodium and ammonium salts **3b** and **4b′** were prepared and characterized. In different solvents, the presence of disk-like polymeric aggregates was shown by small-angle-neutron-scattering spectroscopy (SANS) and confirmed by transmission-electron microscopy (TEM). Their thickness and radii were determined, and the molecular masses were calculated. Defined structural changes of the polymers were observed during several weeks of storage in saturated DMSO solutions. The polymers **2a′** and **2b′** were stabilized by aggregation (preferentially dimerization) of polymer chains. Both aggregation and tautomerization were reversible upon dilution. Ferromagnetism and paramagnetic absorption of previously described CH_2-bridged indigo polymers [6] could not be corroborated for the similarly structured polymer **2b**.

2. Results and Discussion. – 2.1. *Preamble.* Two statistical copolymers consisting of indigo and *N*-acetylindigo building blocks were investigated. The units are connected at the 5,5′-positions either directly (see **2a**) or through a CH_2 group as spacer (see **2b**). The polymers exhibit properties that differ significantly from those of the monomeric equivalents indigo (**1a**) [11] and *N*-acetylindigo (**1b**) [12], and from previously described indigo polymers [4–6].

As known, the typical characteristics of indigo (**1a**) such as high melting point, low solubility, and bathochromic shift of the color band are the result of strong intermolecular association of neighboring *trans* indigo molecules with keto structure due to H-bonds between NH and C=O groups [11]. Indigo compounds with tautomeric

---

[1]) ‘Primes’ are used in two different contexts: for trivial atom numbering (see *Fig. 1*,*b*), and as part of the (bold printed) compound numbers. For example, **2a′**/**2b′** represent the tautomeric forms of **2a**/**2b** and **2a″**/**2b″** the tautomeric and deacetylated forms of **2a**/**2b** (see *Fig. 1*,*b*).

indoxyl/indolone structure are highly uncommon [13]. An exception is the isoelectronic N-atom analog of indigo, indigo-diimine [14].

To the best of our knowledge, no X-ray analyses of the reddish-purple *N*-acetylindigo (**1b**) or the red *N*,*N*′-diacetylindigo (**1c**) [15] have been published. Therefore, that of *N*-(chloroacetyl)indigo (= *N*-(chloroacetyl)-2,2′-biindolinylidene-3,3′-dione = 1-(chloroacetyl)-2-(1,3-dihydro-3-oxo-2*H*-indol-2-ylidene)-1,2-dihydro-3*H*-indol-3-one) was used for comparative interpretations [16]. Although different bond lengths indicate unsymmetrical conjugation of the chromophore, the central C=C bond is retained confirming the keto structure of the molecule.

2.2. *Syntheses.* The syntheses of the polymers **2a** and **2b** are equivalent to those previously employed for the preparation of monomeric [17] and polymeric [5c,d][6a] indigo dyes (*Scheme*). The key step was the repeated oxidative coupling [18] of the reactive 1,1′-diacetyl-3,3′-dihydroxybis-indoles **5** obtained from 1,1′-diacetyl-3,3′-bis-(acetyloxy)bis-indoles **6** through transesterification. In contrast to former preparations, we performed the polymerization process throughout under homogeneous conditions using highly diluted solutions of the starting materials **6** in EtOH (*ca.* 4 mM) with some CH_2Cl_2 as co-solvent. The reactive species were gradually acquired by sequential addition of aqueous NaOH solution, while the mixture was heated under reflux and air-bubbling. The starting volume was kept constant, evaporated solvent was replaced by H_2O. The copolymers **2a** and **2b** were formed by gradual hydrolysis of the red primary products **7a** and **7b**, and **8a** and **8b** (higher acetylated polyindigos) as green and blue solutions, respectively, of their polyanions. After acidification with aqueous HCl solution, the neutral copolymers were precipitated as well-defined products of high molecular masses (20–30% yield). Analogously, *N*-acetylindigo (**1b**) was formed by gradual hydrolysis of *N*,*N*′-diacetylindigo (**1c**).

Due to cleavage of the central C=C bonds of **7**, the hitherto unknown *N*,*N*′-diacetylbis-anthranilic acids **9** were formed as by-products. A similar degradation of the indigo skeleton is described for *N*,*N*′-diacetylindigo (**1c**) and indigo (**1a**) giving *N*-acetylanthranilic acid [19a] and anthranilic acid [19b], respectively (anthranilic acid = 2-aminobenzoic acid).

The tetraacetyl-substituted dihydroxybis-indoles **6a** [5d] and **6b** [6a] were accessible from the tetracarboxylic acids **10a** and **10b**, respectively, by ring closure in boiling Ac_2O/AcONa. The acid **10a** was prepared by alkylation of benzidinedicarboxylic acid **11** with $ClCH_2CO_2H$ [5d]. The benzidine derivative **11** was obtained from 2-nitrobenzoic acid **12** through reduction with Zn in alkaline solution, followed by benzidine rearrangement [20]. The CH_2-bridged tetraacid **10b** was synthesized from *N*-(2-carboxyphenyl)glycine (**13**) and HCHO [1a]. The acid **13** was prepared by alkylation of anthranilic acid (**14**) [21].

2.3. *Properties in Solid State. Color and Composition.* The freshly precipitated polymers **2** form voluminous gelatine-like masses, green for **2a**, and blue for **2b**. After drying, they give amorphous, dark-colored solids with about 0.5 Ac groups and 2 (for **2a**) and 1.5 (for **2b**) molecules of H_2O per monomeric unit. This is similar to a previously described polyindigo [5d].

Thermal Stability. Investigations by means of differential-scanning calorimetry/thermogravimetric analysis (DSC/TGA) reveal higher thermal stabilities for **2** as compared to the monomeric equivalents **1** (dec. 601° for **2a** and 553° for **2b**; dec. 438°

Scheme. a) *Synthesis of Statistical Copolymers* **2a** *and* **2b**. b) *Preparation of the Precursors* **6a** *and* **6b**.

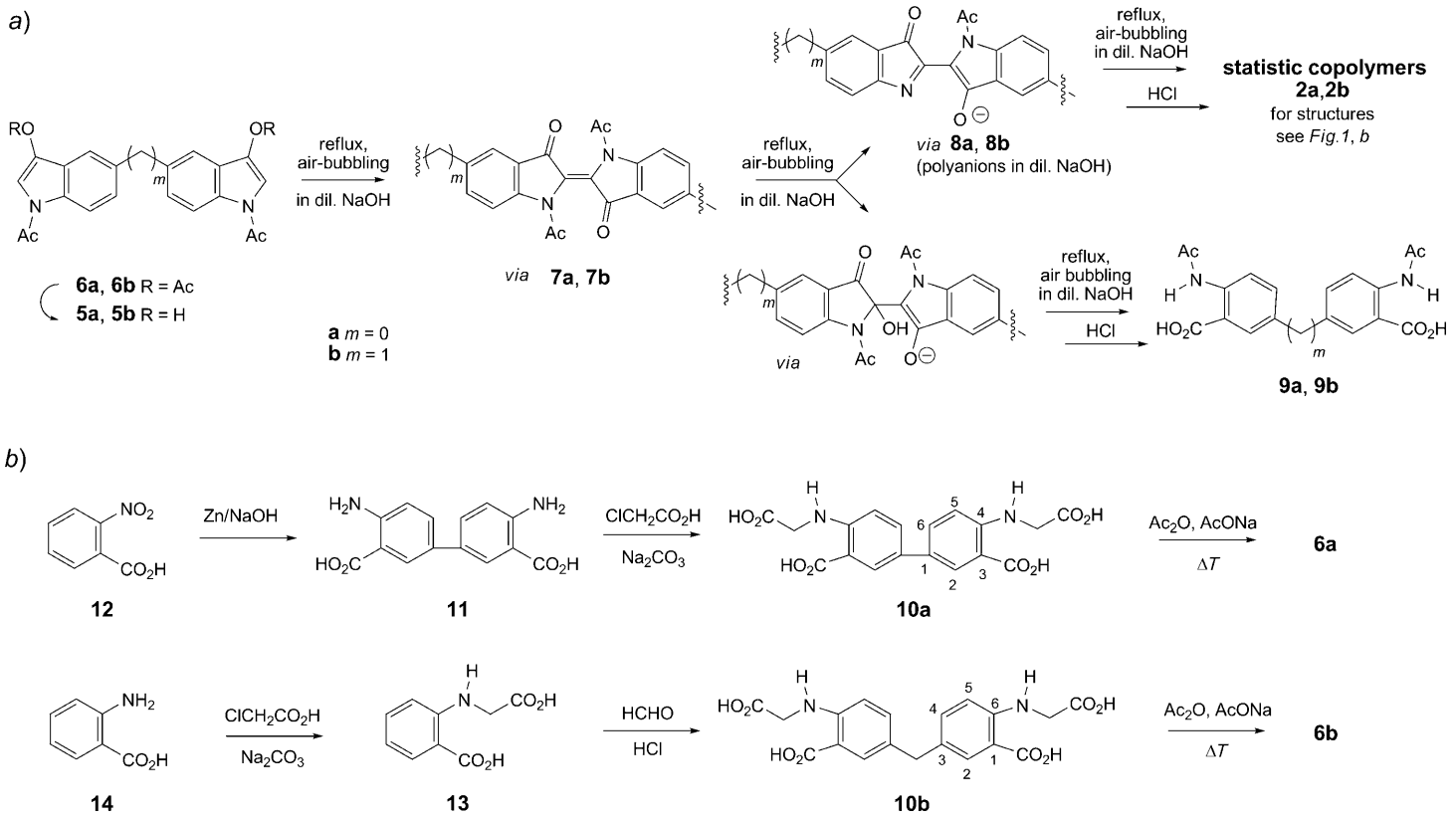

for **1a** [22] and 185–186° for **1b** [12c]). At temperatures up to 450°, the polymers show a continuous, slow loss of weight corresponding to the elimination of ketene (originating from Ac groups) and H_2O. For comparison, the previously described polyindigo is stable in air up to 350° [5d].

Solubility. The polymers **2** are almost insoluble in organic solvents and in H_2O. In DMSO (see also [5d]) and in diluted aqueous bases, they are remarkably soluble after some time of exposure to the solvent (3–4 g/l or *ca.* 10 mM of monomeric equivalent).

Infrared Spectra (IR). Higher-frequency NH absorptions of **2** indicate weaker intermolecular H-bonds of the polymers as compared to indigo (**1a**): 3350 cm^{-1} for **2a** and **2b** and 3244 cm^{-1} for **1a**. They show a broad, strong absorption at 3500–2000 cm^{-1} (H_2O and/or OH) and the amide C=O absorption at 1685 cm^{-1}. Low-frequency ring-C=O bands at 1620 cm^{-1} verify the predominance of polar structures. The number of bands is reduced significantly as compared to indigo (**1a**) [22]. Adjacent peaks are merged to broader signals. These observations confirm previous reports regarding polymeric indigo dyes [5e].

^{15}N- and ^{13}C-NMR Spectra. The solid-state ^{15}N-NMR spectrum of **2b** (*Fig. 2*) shows clearly three sharp signals of different intensities. This provides strong arguments for the keto structure of the unsubstituted indigo unit *A*-*A*′ (δ −282.9 for $N(1^{A,A'})$] and for the tautomeric indoxyl/indolone structure of the *N*-acetylindigo unit *B*-*B*′ (δ −250.5 for $N(1^{B})$ and −212.3 for $N(1^{B'})$). For comparison, the ^{15}N-NMR resonance of indigo (**1a**) appears at δ −278.1 (*Fig. 2*).

The solid-state ^{13}C-NMR spectrum of **1a** shows the expected pattern of sharp signals (see *Exper. Part*) [23]. The signals of polymers **2a** and **2b** are broader and not as clearly arranged.

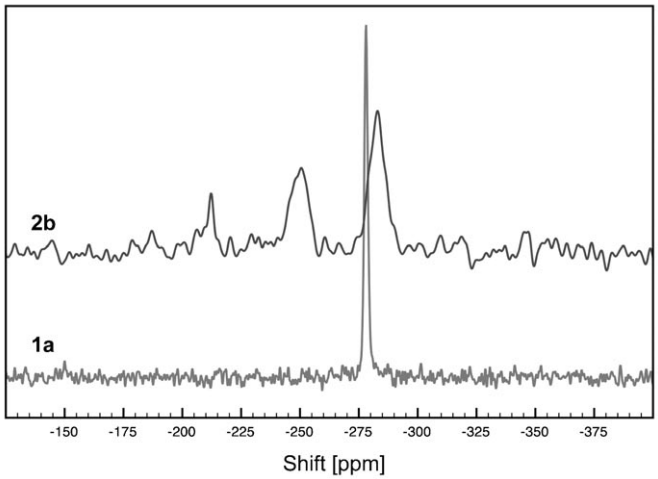

Fig. 2. *Solid-state ^{15}N-NMR spectra of indigo* (**1a**) *and of polymer* **2b**

Mass Spectra (MS). The polymers **2** could neither be characterized by electron-ionization (EI) nor by electro-spray-ionization (ESI) or matrix-assisted laser-

desorption-ionization (MALDI) MS. Some low-molecular fragments with isatine (=1*H*-indole-2,3-dione) end groups were observed by ESI-MS.

Magnetic Properties. In contrast to a previously described 5,5′-CH_2-bridged polyindigo [6], polymer **2b** exhibits no ferromagnetic properties or paramagnetic absorption. However, certain samples prepared by us under less controlled conditions (higher concentrations and/or spontaneous addition of NaOH) are indeed attracted by a permanent magnet (see *Fig. 1,a*). They show a defined hysteresis loop at 40 K which we attribute to some minority phase [24].

2.4. *Properties in Solution. VIS Spectra.* The interaction of directly attached chromophores of polymer **2a** causes a significant red shift of a less intensive, broadened color band (λ_{max} (ε) 660 nm (6000) in DMSO; see *Fig. 3,a*). This is similar to previously described polyindigo [5e] and 5,5′-diaminoindigo dyes [25] and points to a predominantly polar ground-state and to less polar resonance structures in the first exited state (see *Fig. 3,b*). Otherwise, both wavelength and intensity of the color band of the CH_2-bridged polymer **2b** (λ_{max} (ε) 642 nm (12000) in DMSO) are in a range rather typical for indigo dyes. *Beer*'s law was obeyed in a concentration range of 10^{-5} to 10^{-7} M of monomeric equivalents excluding absorption changes by aggregation.

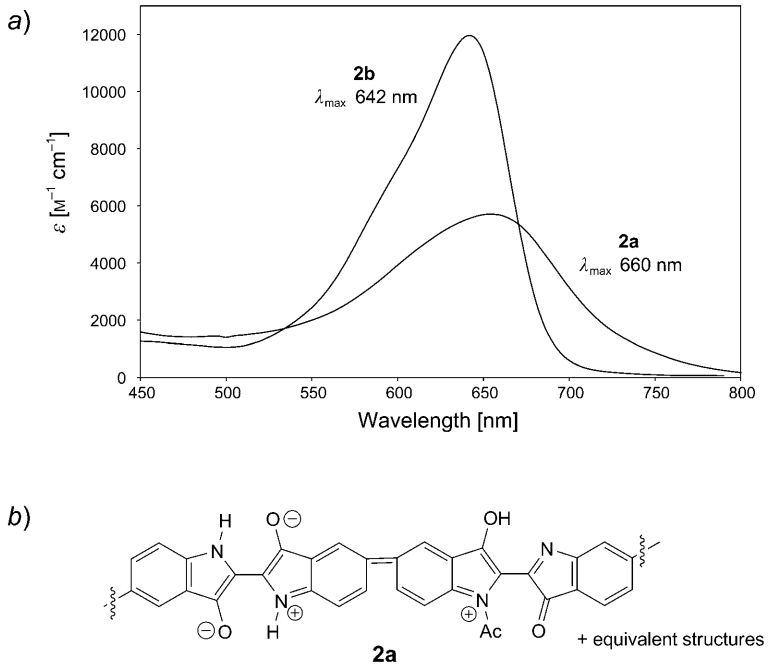

Fig. 3. a) *VIS Spectra of polymers* **2a** *and* **2b** (in DMSO). b) *Representation of the polar ground-state of* **2a**

^{1}H-NMR Spectra. At least the CH_2-bridged polymer **2b** is suitable for ^{1}H-NMR investigations in (D_6)DMSO solutions [26] as suggested by distinct and relatively sharp

resonances. In contrast, the signals of **2a** are weaker and significantly broadened due to hindered dynamics of the polymer chains consisting of directly connected building blocks. The respective signals are throughout the spectrum downfield shifted by 0.1 to 0.3 ppm as compared to **2b**.

The spectra of the polymers confirm the conclusions regarding the structures of the building blocks as derived from the solid-state ^{15}N-NMR spectra. The keto structure of the unsubstituted indigo units *A*-*A*′ is validated by a distinct ^{1}J(N,H) coupling of 108.4 ± 0.5 Hz (for **2b**). The H–N($1^{A,A'}$) signals (δ 10.60 and 10.39) and the upfield-shifted H–C($7^{A,A'}$) signals (δ 7.46 and 7.24) for **2a** and **2b**, respectively, correspond to those of indigo (**1a**) [23]. The tautomeric indoxyl/indolone structure of the *N*-acetylindigo units *B*-*B*′ is verified by the OH–C(3^{B}) signals (δ 11.08 and 10.94) and the downfield-shifted H–C(7^{B}) signals (δ 8.54 and 8.34). The H–C(7^{B}) resonances correspond to those of the starting materials **6**.

The quantity of *N*-acetylindigo units was determined from the intensity ratio of the Ac and H–C($7^{A,A'}$) signals. Due to overlapping of aromatic-proton signals, no distinct resonances could be identified for **2a** and **2b** in the range from δ 7.6–8.1 and δ 7.3–7.6, respectively.

2.5. *Anionic Polymers in Aqueous NaOH. Amorphous Salts* **3b** *and* **4b′**. *Acidity.* The titration of freshly precipitated suspensions of **2** in dilute HCl solution with NaOH indicates mono-deprotonation of *ca.* 50% of the building blocks. Shallow, but distinct turning points of the titration curves around pH 4 are observed for both polymers. The shape is typical for polyelectrolytes where the protons are gradually released with increasing pH. Therefore, distinct pK_a values could not be established. The polymers are slightly more acidic than 1*H*-indol-3-ol (pK_a 10.46 [15]) due to the presence of Ac groups.

^{1}H-NMR Spectra and Deacetylation. Fresh solutions of **2** in 0.1M NaOD do not show any distinct ^{1}H-NMR resonance. The partial deprotonation causes signal broadening due to exchange reactions. However, over a period of about three months storage of the samples, complete deacetylation occurs, and the slightly blue solutions of the polyanions **2a″** and **2b″** are evident. Their ^{1}H-NMR spectra show signal reduction due to *de facto* symmetrical structures. Three sharp aromatic-proton signals are observed. Especially the H–C(7,7′) signals are highly upfield-shifted (δ 6.88 and 6.73) comparable to the H–C(7^{A}) shift of ammonium salt **4b′**. Attempts to force the acetate hydrolysis at elevated temperatures failed. Instead, hydrolytic cleavage of indigo units resulted in yellow solutions. The neutral deacetylated polymers **2a″** and **2b″** did not precipitate after acidification.

VIS Spectra. Through deprotonation of **2a**, neither the position nor the intensity of the color band is significantly changed (λ_{max} (ε) 657 nm (4600) in 0.1M NaOH). This is probably caused by similar electronic structures of the neutral and the anionic polymers derived from **2a**. To the contrary, the intensity of the somewhat blue-shifted color band of the anionic polymer derived from **2b** is strongly reduced (λ_{max} (ε) 627 nm (2700) in 0.1M NaOH). *Beer*'s law was obeyed in a concentration range of 10^{-5} to 10^{-7} M of monomeric equivalents excluding absorption changes by aggregation.

Amorphous Salts **3b** *and* **4b′**. The sodium and the ammonium salts **3b** and **4b′** were isolated as amorphous hydrates. The results of the combustion analysis indicate the presence of *ca.* 6 and 2.5 molecules of H_2O per monomeric unit for **3b** and **4b′**,

respectively. The salts exhibit characteristic ^{1}H-NMR spectra in (D_6)DMSO. The signal pattern of **3b** correlates to that of the neutral polymer **2b** with the characteristic H–N($1^{A,A'}$) signal of the keto-structured building blocks. The OH–C(3^B) signal is missing, the proton being replaced by Na^+. To the contrary, the ammonium salt **4b′** shows neither NH nor OH resonances but a highly upfield-shifted H–C(7^A) signal (δ 6.64). This points to a structure similar to **2b′** where both acidic protons are replaced by NH_4^+ (see *Fig. 1*, *b*).

The differences may originate from the preparation of the materials. The gelatine-like sodium salt **3b** was dried under neutral conditions allowing protonation to give the keto-structured *A*-*A′* building blocks. In contrast, the ammonium salt **4b′** was isolated by straight evaporation of its basic solution in aqueous ammonia.

2.6. *Structural Changes and Formation of Dimeric Chains of* **2a′** *and* **2b′**. The ^{1}H-NMR spectra of **2a** and **2b** indicate clearly distinct, time depending structural changes over a period of about six months storage in saturated (D_6)DMSO solutions (*ca.* 10 mM of monomeric units). The keto structure of the unsubstituted *A*-*A′* building blocks reverts to the tautomeric indoxyl/indolone structure in **2a′** and **2b′** (*Fig. 4*, *a*). Consequently, the significant H–N($1^{A,A'}$) and H–C($7^{A,A'}$) resonances of **2a** and **2b** are gradually decreasing in favor of OH–C(3^A) and H–C(7^A) signals of **2a′** and **2b′** (see *Fig. 4*, *b*–*d*). The new polymer chains are stabilized by aggregation. Intermolecular H-bonds may cause the required energy gain to establish the tautomeric building blocks at the cost of intramolecular H-bonds present in the former keto-structured units. The central single bonds of **2a′** and **2b′** seem to afford more flexibility of the polymer chains and thus less energy requirement for positioning towards aggregation.

The aggregation/tautomerization was followed by optical spectroscopy of freshly diluted, aggregate-containing samples too. The color bands λ_{max} of **2a** (660 nm) and **2b** (642 nm) are shifted to 634 and 725 nm (sh) for **2a′** and **2b′**, respectively, during 6 months. Whereas the blue-shifted color band of **2a′** does not display significant optical characteristics, the red-shifted absorption of **2b′** indicates species with *J*-type (coplanar) orientation of the chromophores similar to indigo (**1a**) [27]. Both aggregation and tautomerization of the polymers are reversible. After a few minutes following dilution of aggregate containing samples of **2a′** and **2b′**, alterations of the optical spectra are evident (*Fig. 5*). And within 10 h, the original absorptions of **2a** and **2b** are almost reestablished (see Fig. *5*, *b* and *c*, resp.). Complete recovery is prevented by partial degradation [28]. The spectral evolution for both polymers during disaggregation reveals distinct isosbestic points. Consequently, the aggregation of polymer chains was likely a clean process leading to formation of dimers [27].

2.7. *X-Ray Powder Diffraction of Polymeric Salts.* The goal of the study of polymeric salts **3b** and **4b′** was to examine structural features in X-ray powder-diffraction experiments. The diffraction from both salts is heavily influenced by diffuse scattering as well as some effects for the beam-stop that have also been observed in the lowest 2θ region. However, beside these influences, some low ordered structural features of the component polymer can still be seen from the diffraction diagrams (see *Fig. 6*). In the diffraction pattern of the ammonium salt **4b′**, the first broad peak at $d = 14.67$ Å is probably a result of repetition of monomeric units, although the calculated monomer length of 13.90 Å is slightly less (length of **1a**, 12.49 Å [11b] plus one C–C bond, 1.41 Å). One possible explanation for this difference is the elongation of the central

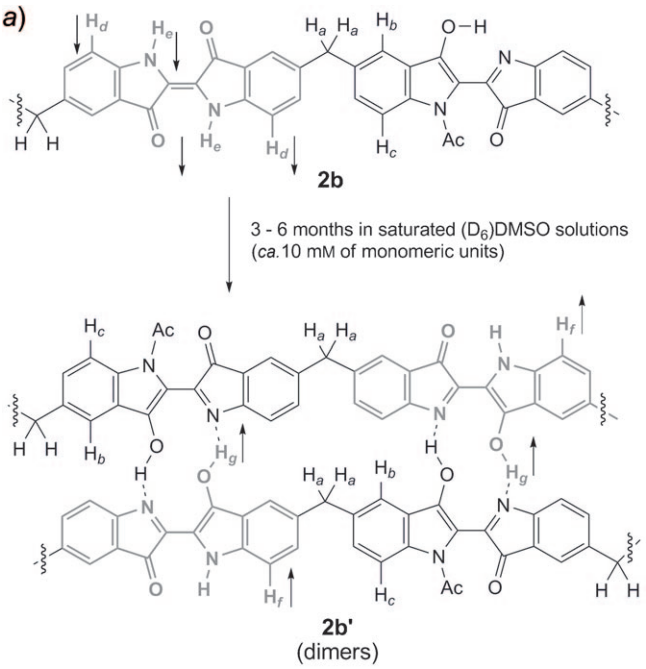

Fig. 4. a) *Slow structural changes of polymer* **2b** (decreasing ^{1}H-NMR-signal intensities) *to give H-bridged dimers of* **2b′** (increasing ^{1}H-NMR-signal intensities) *as followed by* ^{1}*H-NMR spectra* (3–6 months, *ca.* 10 mM of monomeric units in (D_6)DMSO); polymer **2b** ($\delta(H_d)$ 7.24 and $\delta(H_e)$ 10.39) → dimers of **2b′** ($\delta(H_f)$ 6.83 and $\delta(H_g)$ 10.96)). b) ^{1}*H-NMR Spectrum of a fresh sample of* **2b**. c) ^{1}*H-NMR Spectrum of the same sample after 3 months of storage, and* d) *after 6 months of storage.*

bonds of the monomeric units of **4b′**. The *d* values of 7.72 and 4.00 Å can be related approximately to one half and one quarter of the length of the monomer. However, the *d* value of 5.49 Å does not originate from the repetition of any fraction of the monomer but is probably related to intermolecular spacing between two consecutive monomers, which is calculated from the reported structure of indigo (**1a**) [11b] and found to be 5.77 Å. The broad peaks found in the diffraction pattern of the sodium salt **3b** can be explained by similar considerations. The strong peak at $2\theta = 58.38°$ for both samples probably originates from some residual inorganic material with a small unit-cell volume.

2.8. *Estimation of the Molecular Mass by Hydrodynamic Experiments.* For polymer **2b**, a high molecular mass of well above 10^6 g/mol was established by gel-permeation chromatography (GPC). GPC was performed with solutions of **2b** and indigocarmine (5,5′-disulfonic acid disodium salt of **1a**) in 0.1M NaOH. As standards cobalamin (*M* 1382 g/mol) and blue dextran (*M* $2 \cdot 10^6$ g/mol) were used. Elution of polymer **2b** was observed in the range of blue dextran indicating a size-exclusion volume of well above 10^6 g/mol. Under the same conditions, indigocarmine elutes with cobalamin. Differential ultracentrifugation (differential UC) in 0.1M NaOH (pelletation) as well as UC with a sucrose gradient (comparatively broad blue band) confirmed the mass estimate

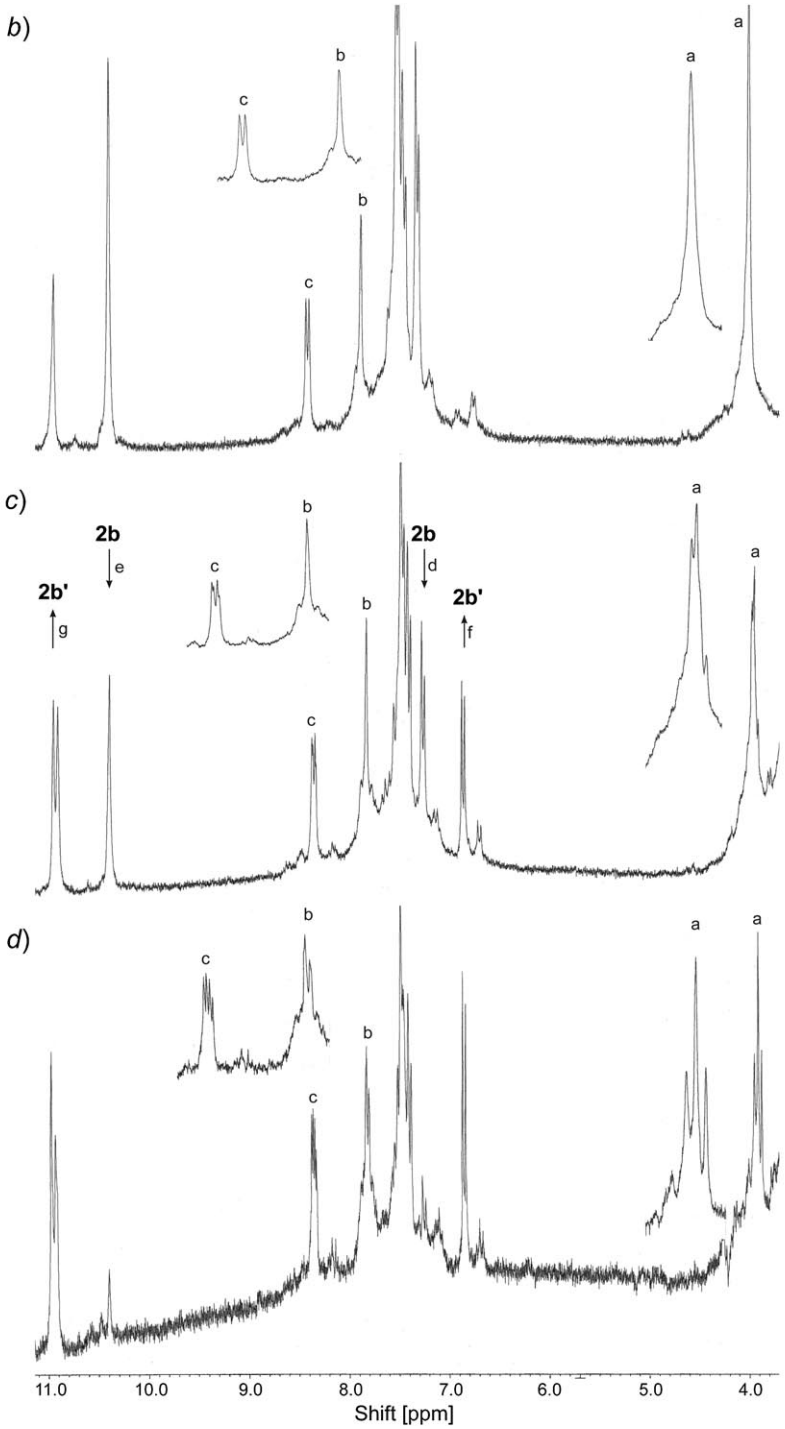

Fig. 4 (cont.)

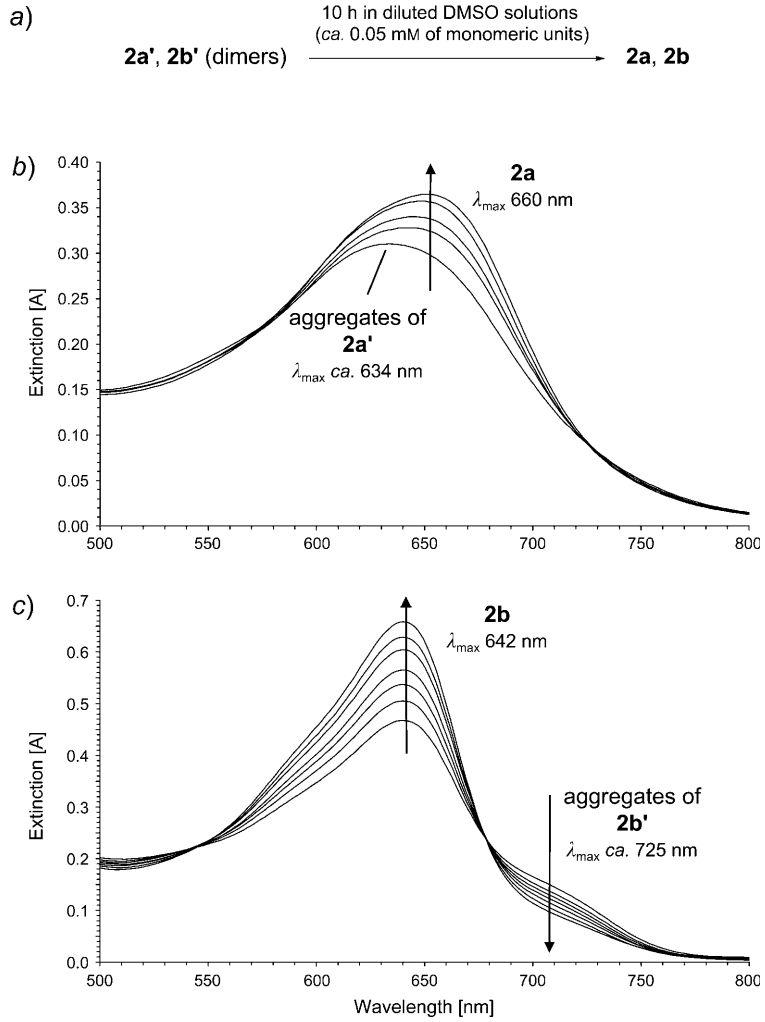

Fig. 5. a) *Time-depending disaggregation of dimeric* **2a′** *and* **2b′** *upon dilution to give* **2a** *and* **2b**, *respectively, as followed by VIS spectra* (10 h, *ca.* 0.05 mM of monomeric units in DMSO). b) *Dimers of* **2a′** (λ_{max} 634 nm) → *polymer* **2a** (λ_{max} 660 nm). c) *Dimers of* **2b′** (λ_{max} 725 nm, sh) → *polymer* **2b** (λ_{max} 642 nm)

for **2b**. The results confirm **2b** as a polymer that could be in an aggregated form. They motivated us to further structural analyses by small-angle-neutron-scattering (SANS), transmission-electron microscopy (TEM), and dynamic-light-scattering (DLS) experiments.

2.9. *Mesoscopic Structural Characterization.* As a first step, the density ϱ of the polymers was determined by UC on a sucrose gradient to be 1.218 g/cm^3 and 1.210 g/cm^3 for **2a** and **2b**, respectively (see *Fig. 7*). The density of crystalline indigo (**1a**) is

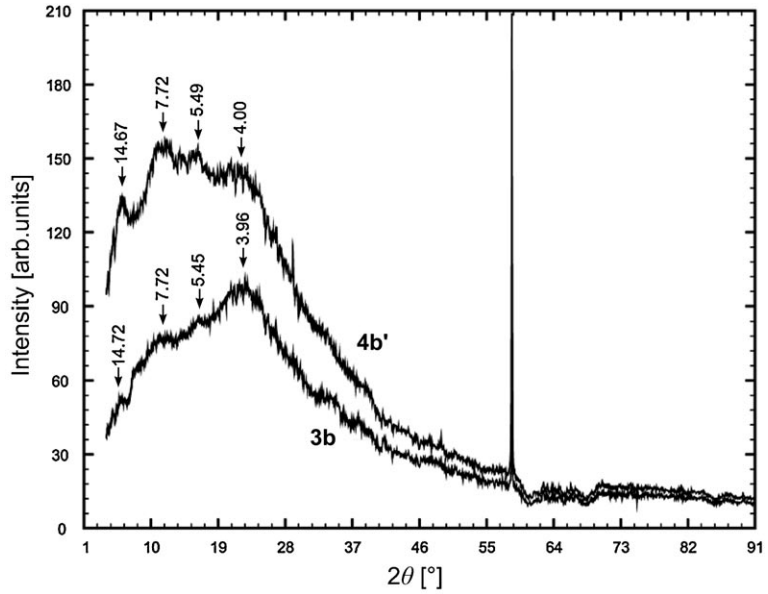

Fig. 6. *X-Ray powder diffraction pattern for* **3b** *and* **4b′** *zoomed over the 2θ range 4–91°*. The positions of the broad peaks are shown by arrows, and the corresponding *d* values are in Å.

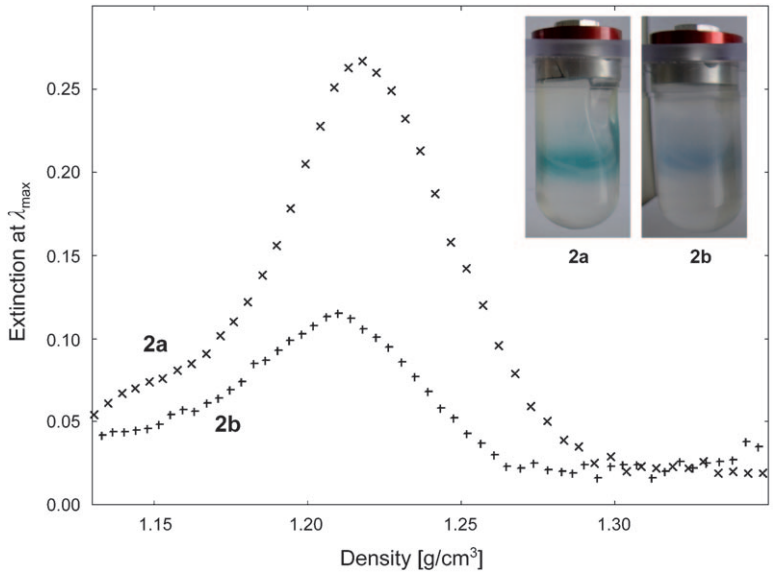

Fig. 7. *Ultracentrifugation of* **2a** *and* **2b** *on a 30–70% sucrose gradient in 0.1*M *NaOH: Density distribution* ϱ [g/cm^3] *of* **2a** (×) *and* **2b** (+) *as a function of the extinctions at positions of the color bands* (E at λ_{max}). Photograph after centrifugation.

1.48 g/cm^3 [29], and of polymeric indigo dyes 1.3 – 1.5 g/cm^3 [5a], thus the values for the polymers are in the lower range of densities for such systems.

For SANS measurements, nearly saturated solutions of neutral polymers in (D_6)DMSO, and from incompletely deprotonated polymers in 0.1M NaOD (2.3 – 3.6 g/l, see *Table*) were used. In *Fig. 8*, the scattering intensity I is given as a function of the

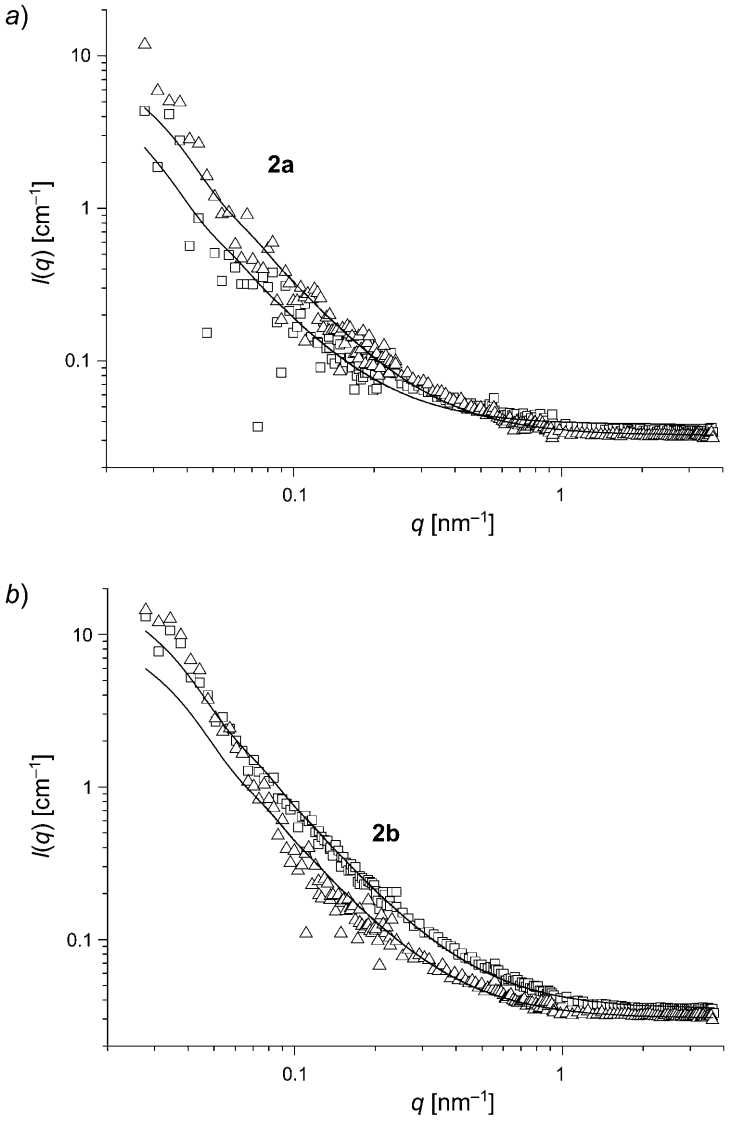

Fig. 8. *SANS Intensities for* a) *polymer* **2a** (in 0.1M NaOD (□) and in (D_6)DMSO (△)) *and* b) *polymer* **2b** (in 0.1M NaOD (□) and in (D_6)DMSO (△)) *as a function of the magnitude of the scattering vector* q *at 25°*. Solid lines are fitted curves according to *Eqns. 3* and *4*.

Table. *Structural Parameters Obtained from the SANS Analysis.* Radius of gyration R_g and molecular mass M (I_0), obtained from the *Guinier* analysis, and radius R, thickness D, and M obtained from fitting the disk model to the data.

	2a (NaOD/D_2O)	**2a** ((D_6)DMSO)	**2b** (NaOD/D_2O)	**2b** ((D_6)DMSO)
c [g/l]	2.33	3.55	3.0	3.45
R_g [nm]	33.9	35.3	28.0	30.7
M (I_0) [g/mol]	$1.57 \cdot 10^6$	$6.8 \cdot 10^6$	$3.6 \cdot 10^6$	$9.0 \cdot 10^6$
R [nm]	82.5	73.9	68.4	70.2
D [nm]	0.20	0.27	0.34	0.35
M [g/mol]	$1.53 \cdot 10^6$	$3.6 \cdot 10^6$	$3.6 \cdot 10^6$	$3.9 \cdot 10^6$

magnitude q of the scattering vector. These data confirm the presence of large colloidal aggregates in both basic aqueous solution as well as in DMSO for polymers **2a** and **2b**. In general, the scattering curves look similar for both polymers and in both solvents. They exhibit a continuous increase of I towards low q and a relatively weak scattering at large q, which can be interpreted such that there are no structural repeating units in the nm range. A pronounced intensity increase in the low q range is observed that does not yet level off toward a constant value and thereby indicates the presence of rather large aggregates.

For a first analysis of the SANS results, the *Guinier* approximation of *Eqn. 1* was used [30] for the intensity data in the low q range ($q < 0.07\ \mathrm{nm}^{-1}$). From this approximation, we deduced the radius of gyration, R_g, of the aggregates present and the intensity at zero-scattering angle, I_0, to characterize the mesoscopic structure present in these solutions. From I_0 the effective molecular mass M_{eff} of the aggregates can be calculated by *Eqn. 2*, where ϱ_{agg} is the density of the polymers, c_g the mass concentration, and SLD_{agg} and SLD_0 the scattering length and densities of polymers and solvent, respectively. In the case of polymers **2a** and **2b**, they are for D_2O $27.4 \cdot 10^9$ and $28.8 \cdot 10^9\ \mathrm{cm}^{-2}$, and for (D_6)DMSO $52.8 \cdot 10^9$ and $63.6 \cdot 10^9\ \mathrm{cm}^{-2}$, respectively. The obtained data are summarized in the *Table*. It should be noted that the values for both molecular mass and radius of gyration R_g are only lower limits as it was not possible to guarantee sufficiently low q values for comfortable *Guinier* limits. However, it is clear from the performed analysis that the solutions contain definitely relatively large aggregates with molecular masses well above 10^6 g/mol. In addition, it is interesting to note that for both indigo polymers the molecular mass of their aggregates is always somewhat larger for the solutions in (D_6)DMSO compared to those in 0.1M basic D_2O solution. This further indicates that we do not observe the scattering of individual polymers but rather of aggregates of such polymers.

$$I(q) = I_0 \cdot \exp\left(-\frac{q^2 \cdot R_g^2}{3}\right) \tag{1}$$

$$M_{eff} = I_0 \cdot \frac{N_{Av} \cdot \varrho_{agg}^2}{c_g \cdot (SLD_{agg} - SLD_0)^2} \tag{2}$$

The scattering curves show a characteristic slope of q^{-2} in the low q range, which is typical for flat structures. Therefore, we fitted our data with a model of homogeneous

disks, for which the scattering intensity is given by *Eqn. 3* [30][31], where ^1N is the number density of the aggregates, V their volume, Δr the difference of the scattering length densities of solvent and aggregate, and $P(q)$ the form factor of the aggregates, that for randomly oriented disks of radius R and thickness D is given by *Eqn. 4* [32].

Therein, J_1 is the *Bessel* function of 1st order. In addition, we also accounted for the experimental wavelength distribution of 11% FWHM (full width at half maximum) by smearing into in the fitting procedure the theoretically calculated curves (*Eqns. 3* and *4*) with a triangular wavelength distribution of 11% FWHM.

$$I(q) = {}^1N \cdot V^2 \cdot \Delta\varrho^2 \cdot P(q) \tag{3}$$

$$P(q,R,D) = \int_0^{\pi/2} \left\{ \left[\frac{2J_1(qR\sin\phi)}{qR\sin\phi} \right] \left[\frac{\sin((qD/2)\cos\phi)}{(qD/2)\cos\phi} \right] \right\}^2 \sin\phi d\phi \tag{4}$$

This analysis provides very good fits to the absolute intensity of the scattering data (shown as solid lines in *Fig. 8*, *a* and *b*). The fitted parameters are summarized in the *Table* and show that the radii R of the disk-like aggregates are always in the range of 70–80 nm. The obtained thickness D is 0.2–0.4 nm, *i.e.*, the sheets are just of one-molecular thickness. From the disk volume, the molecular mass of the aggregates can be calculated, and in particular for the samples in 0.1M NaOH, they are in very good agreement with those obtained by the *Guinier* analysis, while somewhat lower values are found for the solutions in (D_6)DMSO. The formation of disks can be explained by a structural arrangement in which the indigo polymers form flat sheets in which polymer molecules are directly associated to their neighboring molecules, thereby forming extended sheets, as for instance observed in amyloid self-assemblies [33].

The presence of disk-like aggregates is well corroborated by the electronmicrographs obtained by transmission-electron microscopy (TEM) (*Fig. 9*) after drying a solution of **2b** on a grid. Here, we see clearly elongated objects with lengths up to ca. 200 nm. This coincides very well with the diameter of the disks obtained from the SANS experiments. In TEM, such disks will show up mostly when viewed from the side because in the view oriented with their face to the electron beam – a thickness of only 0.3 to 0.4 nm – they will appear almost transparent. Accordingly, we can only observe disks when they are substantially tilted or are totally or partially involuted. However, the structural picture is in quantitative agreement with the structural parameters deduced by the disk model from the SANS data which was further confirmed by dynamic light-scattering measurements that yielded hydrodynamic radii of 62.4 nm and 29.4 nm for indigo polymer **2a** and **2b**, respectively, in 0.1M NaOH.

3. Conclusions. – Two statistical copolymers are investigated consisting of 5,5′-connected indigo and *N*-acetylindigo units. The building blocks are either directly joined or connected through a CH_2 bridge as a spacer. Methods controlling the polymerization process were developed to obtain homogeneous and well-defined products of high molecular masses. The polymers are soluble in DMSO and – incompletely deprotonated – in diluted aqueous bases. They consist of indigo units with keto structure and *N*-acetylindigo units with tautomeric indoxyl/indolone structure.

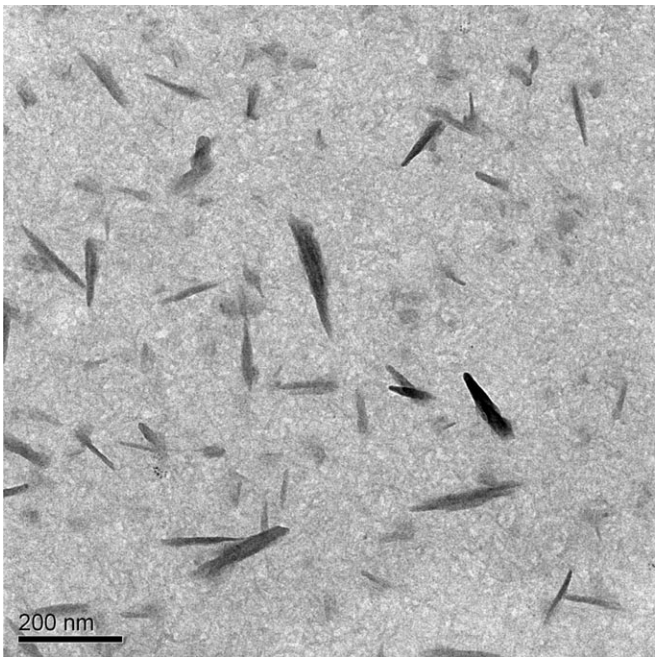

Fig. 9. *Transmission-electron micrograph of a dried sample of* **2b** *in 0.1*M *NaOH*

They form amorphous salts of elongated monomer lengths as compared to monomeric indigo. The polymers were characterized by means of spectroscopic and other physico-chemical methods, in solid state and in solution. For concentrated solutions, evidence for large, disk-like polymeric particles of a thickness of just a few molecular layers was obtained by small-angle neutron scattering (SANS) and confirmed by transmission-electron microscopy (TEM). The molecular masses, calculated from the disk volumes, agree with the ones obtained from the *Guinier* analysis. – During several weeks of storage in concentrated DMSO solutions, defined structural changes of the polymers are observed. The newly formed polymers consist throughout of building blocks with the more flexible, tautomeric indoxyl/indolon structure, probably simultaneously stabilized by intermolecular H-bonds through formation of dimers. Both aggregation and tautomerization are reversible upon dissolution.

The authors thank Dr. *O. Meyer*, Dr. *G. Platz*, Dr. *F. X. Schmid*, Dr. *S. Prevost*, and Dr. *V. Svetlitchny* for experimental support. Many years of scientific friendship and discussions with Dr. *G. Platz* and Dr. *W. Schramm* are gratefully acknowledged. The beam time on the *V4* instrument at the *Helmholtz Zentrum Berlin* (*HZB*) has been supported by the *European Commission* under the 6th framework program through the key action 'Strengthening the European Research Area, Research Infrastructures', contract no. RII3-CT-2003-505925 (NMI3).

Experimental Part

General. All solvents were distilled before use. Column filtration: *Merck* silica gel *60* (SiO_2; 0.040–0.063 mm). Differential scanning calorimetry/thermogravimetric analysis (DSC/TGA): *Netzsch DSC*

200, heating rate 10°/min. VIS Spectra: *Specord 200* (*Analytik Jena AG*); λ_{max} in nm, ε in M^{-1} cm^{-1}. IR Spectra: *Perkin-Elmer Paragon 1000 FT*; $\tilde{\nu}$ in cm^{-1}. NMR Spectra: *Jeol JNM-EX 270* (^{1}H at 270 and ^{13}C at 67.9 MHz), *Bruker DRX 500* (^{1}H at 500 MHz), and *Bruker Avance II* (^{13}C at 75.5 MHz and ^{15}N at 30.4 MHz); δ(H) and δ(C), and δ(N) in ppm rel. to Me_4Si and $MeNO_2$ as internal standard, resp., *J* in Hz; rel. signal intensities for polymers refer to one monomer unit. assignments supported by *J*mod, H,H-COSY, and HMQC-COSY experiments. MS: EI with *Varian-MAT-312* at 70 eV and LCT ESI-TOF with *Micromass* spectrometer; in *m*/*z* (rel. %). Elemental analysis: *Vario EL III* (*Elementar*).

General Procedure A (*GP A*). A stirred suspension of **10** (1 equiv.), Ac_2O (5 equiv.), and AcONa (anh., 25 equiv.) was heated under reflux to 170° and kept boiling for 30 min. After cooling, the mixture was concentrated, the residue taken up with toluene and again concentrated. The procedure was repeated several times. The final residue was extracted with CH_2Cl_2. After evaporation of all volatiles, the crude product was dissolved in CH_2Cl_2 and filtered through the 50-fold amount of SiO_2 with toluene/AcOEt 4:1: 19–24% of **6**.

General Procedure B (*GP B*). To a stirred soln. of **6** (1 mmol) in CH_2Cl_2 (25 ml), EtOH (250 ml) was added. Upon heating under reflux and air-bubbling, 1M NaOH (15 ml) was added in five portions during 5 h. Heating and air-bubbling was continued for 5 h. The starting volume was maintained, evaporated solvent was replaced by H_2O. After addition of 1M HCl (30 ml) to the colored soln. ($pH \leq 2$), the gelatine-like precipitate was collected by centrifugation (20 min, 10000 rpm), washed with H_2O, EtOH, and Et_2O, and dried for 16 h at 30°/0.005 Torr: 19–29% of **2**. Evaporation of the EtOH supernatant gave 32–37% of **9**.

General Procedure C (*GP C*). Dimers of **2a′** and **2b′** were formed within 3–6 months storage of conc. solns. of **2a** and **2b**, resp., in (D_6)DMSO at r.t.

General Procedure D (*GP D*). The polyanions of **2a″** and **2b″** were formed within 3 months storage of **2a** and **2b**, resp., in 0.1M NaOD at r.t.

General Procedure E (*GP E*). Polymer **2** (*ca.* 0.3 mmol) was dissolved in 0.1M NaOH (25 ml, 2.5 mmol). After 24 h storage at r.t., 1M HCl (3.0 ml, 3.0 mmol) was added ($pH \leq 2$). Titration was performed with 0.1M NaOH (pH electrode *HI 9321*, *HANNA Instruments*).

Benzidine-3,3′-dicarboxylic Acid (*=4,4′-Diamino[1,1′-biphenyl]-3,3′-dicarboxylic Acid*; **11**). Prepared according to [20b] from 2-nitrobenzoic acid (**12**). DSC/TGA: (234) 292° (dec.) ([20a]: 300°). ^{1}H-NMR (270 MHz, (D_6)DMSO): 7.27 (*d*, ^3J = 8.4, 2 H, H–C(5,5′)); 7.75 (*dm*, ^3J = 8.4, 2 H, H–C(6,6′)); 8.04 (*sm*, 2 H, H–C(2,2′)); 8.89 (NH_2, CO_2H). ^{13}C-NMR (67.9 MHz, (D_6)DMSO): 116.8; 121.3; 128.9; 131.6; 131.9; 143.1; 168.8.

N,N-*Bis(carboxymethyl)benzidine-3,3′-dicarboxylic Acid* (*=4,4′-Bis[(carboxymethyl)amino]-[1,1′-biphenyl]-3,3′-dicarboxylic Acid*; **10a**). The acid **10a** was prepared from **11** and $ClCH_2CO_2H$ according to [5d]. DSC/TGA: (180) 221° (dec.) ([5d]: 230–232°). ^{1}H-NMR (270 MHz, (D_6)DMSO): 4.04 (*s*, 2 CH_2); 6.68 (*d*, ^3J = 8.8, 2 H, H–C(5,5′)); 7.71 (*dm*, ^3J = 8.8, 2 H, H–C(6,6′)); 7.99 (*sm*, 2 H, H–C(2,2′)). ^{13}C-NMR (67.9 MHz, (D_6)DMSO): 44.9; 111.6; 113.1; 127.0; 128.5; 132.5; 149.2; 169.9; 172.3.

6,6′-Bis[(carboxymethyl)amino]-3,3′-methanediyldibenzoic Acid (*=3,3′-Methylenebis[6-[(carboxymethyl)amino]benzoic Acid]*; **10b**). The acid **10b** was prepared from **13** and HCHO according to [1a]. DSC/TGA: (205) 260° (dec.) ([1a]: 206–207°). R_f 0.56 (AcOEt/AcOH 99:1). IR (KBr): 3375, 1700, 1680. ^{1}H-NMR (270 MHz, (D_6)DMSO): 3.69 (*s*, 1 CH_2); 3.95 (*s*, 2 CH_2); 6.53 (*d*, ^3J = 8.5, 2 H, H–C(5,5′)); 7.20 (*dd*, ^3J = 8.5, ^4J = 2.2, 2 H, H–C(4,4′)); 7.61 (*d*, ^4J = 2.2, 2 H, H–C(2,2′)). ^{13}C-NMR (67.9 MHz, (D_6)DMSO): 39.3; 44.6; 110.9; 112.4; 128.4; 131.8; 135.5; 148.9; 170.1; 172.3.

*1,1′-Diacetyl-3,3′-bis(acetyloxy)-1*H,*1′*H-*5,5′-biindole* (*=1,1′-Diacetyl-[5,5′-bi-1*H*-indole]-3,3′-diol 3,3-Diacetate*; **6a**). According to *GP A*, with **10a** (4.95 g, 12.7 mmol), AcONa (6.7 g, 82 mmol), and Ac_2O (30.0 ml, 317 mmol). 1.04 g (19%) of **6a**. Pale brownish solid. DSC/TGA: 222.5° (dec.) ([5d]: 211–212°). R_f 0.42 (toluene/AcOEt 4:1). IR (KBr): 3203, 1750, 1699, 1212. ^{1}H-NMR (270 MHz, (D_6)DMSO): 2.42 (*s*, 2 AcO); 2.64 (*s*, 2 AcN); 7.76 (*dm*, ^3J = 8.5, 2 H, H–C(6,6′)); 7.83 (*sm*, 2 H, H–C(4,4′)); 7.94 (*s*, 2 H, H–C(2,2′)); 8.43 (*d*, ^3J = 8.5, 2 H, H–C(7,7′)). ^{13}C-NMR (67.9 MHz, (D_6)DMSO): 21.5; 24.2; 116.3; 117.02 (2C); 124.9; 125.6; 132.5; 134.3; 136.3; 169.0; 170.0. EI-MS: 432 (43, M^+), 390 (52, [$M - C_2H_2O]^+$), 348 (100, [$M - 2\ C_2H_2O]^+$), 306 (92, [$M - 3\ C_2H_2O]^+$), 264 (76, [$M - 4\ C_2H_2O]^+$), 207 (27), 43 (72).

*1,1′-Diacetyl-3,3′-bis(acetyloxy)-5,5′-methanediyl-1*H,*1′*H-*bisindol* (=*5,5′-Methylenebis[1-acetyl-1*H-*indol-3-ol] 3,3′-Diacetate*; **6b**). According to *GP A*, with **10b** (23.93 g, 59.5 mmol), AcONa (31.7 g, 387 mmol), and Ac_2O (140 ml, 1.49 mol): 6.34 g (24%) of **6b**. Pale brownish solid. A sample was recrystallized from toluene. DSC/TGA: 244.2° (dec.). R_f 0.48 (toluene/AcOEt 4:1). IR (KBr): 3200, 1760, 1690, 1200. ^{1}H-NMR (270 MHz, (D_6)DMSO): 2.37 (*s*, 2 AcO); 2.59 (*s*, 2 AcN); 4.14 (*s*, 1 CH_2); 7.25 (*dd*, ^3J = 8.5, ^4J = 1.6, 2 H, H−C(6,6′)); 7.41 (*d*, ^4J = 1.6, 2 H, H−C(4,4′)); 7.87 (*s*, 2 H, H−C(2,2′)); 8.24 (*d*, ^3J = 8.5, 2 H, H−C(7,7′)). ^{13}C-NMR (67.9 MHz, (D_6)DMSO): 21.2; 24.2; 40.9; 116.3; 116.6; 117.9; 124.4; 127.3; 131.7; 134.0; 137.5; 168.8; 169.8. EI-MS: 446 (16, M^+), 404 (52, $[M - C_2H_2O]^+$), 362 (100, $[M - 2\ C_2H_2O]^+$), 320 (95, $[M - 3\ C_2H_2O]^+$), 278 (94, $[M - 4\ C_2H_2O]^+$), 146 (23), 43 (83). HR-MS: 446.1460 (M^+, $C_{25}H_{22}N_2O_6^+$; calc. 446.1478).

Indigo (=*2-(1,3-Dihydro-3-oxo-2*H-*indol-2-ylidene)-1,2-dihydro-3*H-*indol-3-one*; **1a**). ^{13}C-NMR (75.5 MHz, solid state): 113.9 (C(7), C(7′)); 121.0 (C(2), (C(2′), C(3a), C(3′a), C(5), C(5′)); 125.2 (C(4), C(4′)); 135.2 (C(6), C(6′)); 153.3 (C(7a), C(7′a)); 188.7 (C(3), C(3′)). ^{15}N-NMR (30.4 MHz, solid state): −278.08 (N(1), N(1′)).

*Poly[3,3′-dioxo-1*H,*1′*H-*2,2′-biindolylidene-5,5′-diyl with 0.5 (1-Acetyl) and 2 H_2O]* (= $(C_{34}H_{18}N_4O_5 \cdot 4\ H_2O)_{n/2}$), i.e., *Poly[(1,3-dihydro-3-oxo-2*H-*indol-5-yl-2-ylidene)(1,3-dihydro-3-oxo-2*H-*indol-5-yl-2-ylidene)(1-acetyl-3-hydroxy-1*H-*indole-5,2-diyl)(3-oxo-3*H-*indole-2,5-diyl) Hydrate (1:4)]* (**2a** · 4 H_2O), *and 4,4′-Bis(acetylamino)[1,1′-biphenyl]-3,3′-dicarboxylic Acid* (**9a**). According to *GP B*, with **6a** (517 mg, 1.19 mmol) and 1M NaOH (17.9 ml, 17.9 mmol): 109 mg (29%) of **2a** · 4 H_2O. Dark green amorphous solid. DSC/TGA: (410) 600.9° (dec.). Turning point of the titration curve: *ca.* pH 4 (see *GP E*). VIS (DMSO): 660 (6000). VIS (0.1M NaOH): 657 (4600). IR (KBr): 3500 (br.), 3365 (sh, NH), 1686*m* (CONH), 1619*s* (CO), 1467, 1406, 1320, 1185, 1118, 1073, 818, 580. ^{1}H-NMR (500 MHz, (D_6)DMSO): among others 2.14 (*s*, 1.5 H, Ac); 7.46 (br., 1 H, H−C($7^{A,A'}$)); 7.8–8.1 (several signals); 8.18 (br., 0.5 H, H−C(4^B)); 8.54 (br., 0.5 H, H−C(7^B)); 10.66 (br., 1 H, H−N($1^{A,A'}$)); 11.07 (br., 0.5 H, OH−C(3^B)). ^{13}C-NMR (75.5 MHz, solid state): among others 171.0; 187.8. Anal. calc. for $(C_{17}H_{13}N_2O_{4.5})_n$ ($(317.29)_n$): C 64.35, H 4.13, N 8.83; found: C 64.05, H 4.18, N 8.41.

The EtOH supernatant was evaporated: 135 mg (32%) of **9a**. Dark brown solid. DSC/TGA: (120) *ca.* 200° (dec.). IR: 3000 (br.), 1664, 1586, 1497, 1370, 1298, 1220, 787, 672. ^{1}H-NMR (270 MHz, (D_6)DMSO): 2.15 (*s*, 2 Ac); 7.90 (*dd*, ^3J = 8.5, ^4J = 1.5, 2 H, H−C(6,6′)); 8.18 (*d*, ^4J = 1.5, 2 H, H−C(2,2′)); 8.54 (*d*, ^3J = 8.5, 2 H, H−C(5,5′)); 11.06 (*s*, 2 NH); 12.92 (*s*, 2 COOH). ^{13}C-NMR (67.9 MHz, (D_6)DMSO): 25.7; 117.8; 121.2; 128.8; 132.3; 133.0; 140.5; 168.9; 169.7. ESI-TOF-MS: 355.55 ($[M - H]^-$). EI-MS: 356 (0, M^+), 320 (100, $[M - 2\ H_2O]^+$), 278 (30). HR-MS: 320.0792 ($C_{18}H_{12}N_2O_4^+$; calc. 320.0797).

*Dimer of Poly[(3-hydroxy-1*H-*indole-5,2-diyl)(3-oxo-3*H-*indole-2,5-diyl)(1-acetyl-3-hydroxy-1*H-*indole-5,2-diyl)(3-oxo-3*H-*indole-2,5-diyl)]* (**2a′**) *in (D_6)DMSO.* See *GP C*. VIS after 3 months: 640 (3500). VIS after 6 months: 634 (2900). ^{1}H-NMR (270 MHz, (D_6)DMSO): among others 2.14 (*s*, 1.5 H, Ac); 6.99 (*dm*, ^3J = 8.1, 0.5 H, H−C(7^A)); 7.8–8.1 (several signals); 8.16 (*sm*, 0.5 H, H−C(4^B)); 8.54 (*dm*, 0.5 H, H−C(7^B)); 11.05–11.15 (1 H, OH−C(3^B), OH−C(3^A)).

*Poly[(3-hydroxy-(1*D)*-1*H-*indole-5,2-diyl sodium salt (1:1)](3-oxo-3*H-*indole-2,5-diyl)]* (**2a″**) *in 0.1M NaOD.* See *GP D*. ^{1}H-NMR (270 MHz): 6.88 (*d*, ^3J = 8.2, 2 H, H−C(7,7′)); 7.89 (*dd*, ^3J = 8.2, ^4J = 2.3, 2 H, H−C(6,6′)); 7.98 (*d*, ^4J = 2.3, 2 H, H−C(4,4′)).

*Poly[3,3′-dioxo-1*H,*1′*H-*2,2′-biindolylidene-5,5′-diylmethylene with 0.5 (1-Acetyl) and 1.5 H_2O]* (= $(C_{36}H_{22}N_4O_5 \cdot 3\ H_2O)_{n/2}$), i.e., *Poly[(1,3-dihydro-3-oxo-2*H-*indol-5-yl-2-ylidene)(1,3-dihydro-3-oxo-2*H-*indol-5-yl-2-ylidene)methylene(1-acetyl-3-hydroxy-1*H-*indole-5,2-diyl)(3-oxo-3*H-*indole-2,5-diyl)-methylene] Hydrate (1:3)]* (**2b** · 3 H_2O), *and 6,6′-Bis(acetylamino)-3,3′-methanediyldibenzoic Acid* (=*3,3′-Methylenebis[6-(acetylamino)benzoic Acid]*; **9b**). According to *GP B*, with **6b** (447 mg, 1.01 mmol) and 1M NaOH (15.2 ml, 15.2 mmol): 63 mg (19%) of **2b** · 3 H_2O. Dark blue amorphous powder. DSC/TGA: (410) 553.4° (dec.). Turning point of the titration curve: *ca.* pH 4 (see *GP E*). VIS (DMSO): 642 (12000). VIS (0.1M NaOH): 627 (2700). IR (KBr): 3370 (br.), 3360 (sh, NH), 1684*m* (CONH), 1620*s* (CO), 1481, 1404, 1296, 1172, 1118, 1066, 820, 448. ^{1}H-NMR (500 MHz, (D_6)DMSO): among others 2.09 (*s*, 1.5 H, Ac); 3.91 (*s*, 2 H, CH_2); 7.24 (*d*, ^3J = 7.9, 1 H, H−C($7^{A,A'}$)); 7.3–7.6 (several signals); 7.82 (*s*, 0.5 H, H−C(4^B)); 8.34 (*d*, ^3J = 8.6, 0.5 H, H−C(7^B)); 10.39 (*s*, 1 H, H−N($1^{A,A'}$)); 10.86 (*s*, 0.5 H, OH−C(3^B)). ^{1}H-NMR (500 MHz, (D_6)DMSO): 10.39 (*d*, ^1J(N,H) = 108.4 ± 0.5). ^{15}N-NMR

(30.4 MHz, solid state): −282.94 ($N(1^{A,A'})$); −250.54 ($N(1^{B})$); −212.22 ($N(1^{B'})$). ^{13}C-NMR (75.5 MHz, solid state): among others 41.0; 169.8; 187.5. Anal. calc. for $(C_{18}H_{14}N_2O_4)_n$ ($(322.31)_n$): C 67.07, H 4.38, N 8.69; found: C 67.15, H 4.36, N 8.04.

The EtOH supernatant was evaporated: 140 mg (37%) of **9b**. Dark brown solid. DSC/TGA: (120) 210° (dec.). IR: 3000 (br.), 1680, 1589, 1508, 1370, 1300, 1228, 1200, 1100, 800, 750, 650. ^{1}H-NMR (270 MHz, (D_6)DMSO): 2.08 (*s*, 2 Ac); 3.90 (*s*, 1 CH_2); 7.40 (*d*, $^3J = 8.1$, 2 H, H−C(4,4′)); 7.77 (*s*, 2 H, H−C(2,2′)); 8.33 (*d*, $^3J = 8.1$, 2 H, H−C(5,5′)); 10.93 (*s*, 2 NH); 12.94 (*s*, 2 COOH). ^{13}C-NMR (67.9 MHz, (D_6)DMSO): 25.5; 39.7; 117.4; 120.9; 131.4; 134.8; 135.8; 139.5; 168.8; 169.8. TOF-ESI-MS: 393.56 ($[M+Na]^+$). EI-MS: 370 (0, M^+), 334 (85, $[M-2\,H_2O]^+$), 319 (20), 292 (30), 43 (100). HR-MS: 334.0950 ($C_{19}H_{14}N_2O_4^+$; calc. 334.0954).

*Dimer of Poly[3-hydroxy-1*H*-indole-5,2-diyl)(3-oxo-3*H*-indole-2,5-diyl)methylene(1-acetyl-3-hydroxy-1*H*-indole-5,2-diyl)(3-oxo-3*H*-indole-2,5-diyl)methylene]* (**2b′**) *in DMSO.* See *GP C*. VIS after 3 months: 642 (2200), 725 (sh). VIS after 6 months: 642 (1600), 725 (sh). ^{1}H-NMR (270 MHz, (D_6)DMSO): 2.08 (*s*, 1.5 H, Ac); 3.90 (*s*, 2 H, CH_2); 6.83 (*d*, $^3J = 8.1$, 0.5 H, H−C(7^A)); 7.3–7.6 (several signals); 7.82 (*m*, 0.5 H, H−C(4^B)); 8.34 (*m*, 0.5 H, H−C(7^B)); 10.86 (br. *s*, 0.5 H, OH−C(3^B)); 10.96 (*s*, 0.5 H, OH−C(3^A)).

*Poly[(1,3-dihydro-3-oxo-2*H*-indol-5-yl-2-ylidene)(1,3-dihydro-3-oxo-2*H*-indol-5-yl-2-ylidene)-methylene[1-acetyl-3-hydroxy-1*H*-indole-5,2-diyl Sodium Salt (1:1)](3-oxo-3*H*-indole-2,5-diyl)methylene] Hydrate (1:12)]* (= $[Na^+\ (C_{36}H_{21}N_4O_5)^- \cdot 12\,H_2O]_n$; **3b** · 12 H_2O). To a soln. of of **2b** · 3 H_2O (140 mg, 0.43 mmol) in 0.1M NaOH (5 ml) was added H_2O (50 ml). After storage for 16 h at r.t., EtOH (500 ml) was added under stirring. The resulting gelatine-like precipitate was collected by centrifugation (20 min, 10000 rpm), washed several times with EtOH and dried for 16 h at 30°/0.005 Torr: 66 mg (37%) of **3b** · 12 H_2O. Dark blue amorphous powder. IR (KBr): 3386, 1618, 1483, 1375, 1297, 1172, 1118, 1065, 816, 559. ^{1}H-NMR (500 MHz, (D_6)DMSO): 2.09 (*s*, 1.5 H, Ac); 3.92 (*s*, 2 H, CH_2); 7.24 (*d*, $^3J = 7.9$, 1 H, H−C($7^{A,A'}$)); 7.3–7.6 (several signals); 7.81 (*s*, 0.5 H, H−C(4^B)); 8.34 (*d*, $^3J = 8.6$, 0.5 H, H−C(7^B)); 10.39 (*s*, 1 H, H−N($1^{A,A'}$)). Anal. calc. for $(C_{18}H_{22.5}N_2Na_{0.5}O_{8.5})_n$ ($(414.38)_n$): C 52.17, H 5.47, N 6.76; found: C 52.20 H 4.80, N 6.42.

*Poly[(3-hydroxy-1*H*-indole-5,2-diyl Ammonium Salt (1:1)](3-oxo-3*H*-indole-2,5-diyl)methylene[1-acetyl-3-hydroxy-1*H*-indole-5,2-diyl Ammonium Salt (1:1)][3-oxo-3*H*-indole-2,5-diyl)methylene] Hydrate (1:5)]* (= $[2\,NH_4^+\ (C_{36}H_{20}N_4O_5)^{2-} \cdot 5\,H_2O]_n$; **4b′** · 5 H_2O). To a soln. of **2b** · 3 H_2O (66 mg, 0.16 mmol) in 25% aq. NH_3 soln. (2.0 ml) was added H_2O (8 ml) under stirring. After 16 h storage at r.t., all volatiles were evaporated, and the residue dried for 16 h at 30°/0.005 Torr: 80 mg (42%) of **4b′** · 5 H_2O. Dark blue, crooked needles. IR (KBr): 3380, 3175, 3005, 2900, 1618, 1482, 1403, 1369, 1294, 1169, 1117, 1064, 818, 558. ^{1}H-NMR (270 MHz, (D_6)DMSO): among others 2.00 (*s*, 1.5 H, Ac); 3.99, 3.92, 3.84 (3*s*, CH_2, NH_4^+); 6.64 (*d*, $^3J = 8.0$, 0.5 H, H−C(7^A)); 7.2–7.6 (several signals); 7.78 (*s*, 0.5 H, H−C(4^B)); 8.32 (*d*, $^3J = 8.6$, 0.5 H, H−C(7^B)). Anal. calc. for $(C_{18}H_{19}N_3O_5)_n$ ($(357.36)_n$): C 60.50, H 5.36, N 11.76; found: C 61.13, H 4.93, N 10.69.

*Poly[(3-hydroxy-(1*D*)-1*H*-indole-5,2-diyl sodium salt (1:1)](3-oxo-3*H*-indole-2,5-diyl)methylene]* (**2b″**) *in 0.1M NaOD.* See *GP D:* ^{1}H-NMR (270 MHz): 3.74 (*s*, 2 H, CH_2); 6.73 (*d*, $^3J = 8.1$, 2 H, H−C(7,7′)); 7.08 (*dd*, $^3J = 8.1$, $^4J = 1.8$, 2 H, H−C(6,6′)); 7.53 (*d*, $^4J = 1.8$, 2 H, H−C(4,4′)).

X-Ray Powder Diffraction. Nonius-PDS120 diffractometer with Cu$K_{\alpha 1}$ radiation (λ 1.540598 Å), equipped with an incident-beam germanium [Ge(111)] monochromator and a 120° – 2° position-sensitive detector. Samples were sealed in a 0.3 mm glass capillary (*Hilgenberg*). The diffraction pattern at 20° was recorded in transmission mode with a total counting time of 90 and 96 h for **3b** and **4b′**, resp.

Dynamic Light Scattering (DLS). *Brookhaven* goniometer *BI-200SM*, *Coherent Compass 315M* 100 mW laser (wavelengths 522–550 nm), and *Brookhaven* autocorrelator *BI-9000AT*. The hydrodynamic radii of incompletely deprotonated polymers in 0.1M NaOH were determined by DLS experiments to be 62.4 and 29.4 nm for **2a** and **2b**, resp.

Gel-Permeation Chromatography (GPC). FPLC Chromatographic system on *Sephacryl S-200 HR* (*Amersham Biosciences*, Freiburg, Germany). GPC was performed with solns. of indigocarmine (5,5′-disulfonic acid disodium salt of **1a**) and **2b** in 0.1M NaOH. Cobalamin (*M* 1382 g/mol) and blue dextran (*M* $2 \cdot 10^6$ g/mol) were used as standards. Elution of **2b** was observed in the range of blue dextran

indicating a size-exclusion volume of well above 10^6 g/mol. Under the same conditions, indigocarmine eluted with cobalamin.

Differential UC. TH-641 Rotor, 35000 rpm at r.t. Solns. of indigocarmine and **2b** in 0.1M NaOH were centrifuged for 50 h. A dark colored pellet of **2b** was evident on the bottom of the cup. Under the same conditions, indigocarmine did not show pelletation.

Differential UC on a 50% Sucrose Solution. A soln. of polymer **2b** in 0.1M NaOH was charged on a 50% soln. of sucrose in 0.1M NaOH. After 50 and 100 h centrifugation, instead of pelletation, a comparatively broad blue band was present.

Sucrose-Gradient UC. TFT-4590 Rotor, with 94 ml thinwall polyallomer cups, 35000 rpm at 4°. Three cups filled with a 5-step gradient of sucrose (30–70% in 0.1M NaOH) were used. Two of them were charged with polymer solns. in 0.1M NaOH (0.51 mg/10 ml for **2a** and 0.52 mg/10 ml for **2b**). After 47 h ultracentrifugation, each polymer formed one band, green and sharp for **2a**, and blue and slightly broadened for **2b**. After fractionation of the samples from bottom to top, the relative polymer concentrations were determined from the extinctions at the positions of the color bands, and the relative sucrose concentrations from the refractive indices [34]. Assuming a sedimentational equilibrium, the densities ϱ were established for **2a** and **2b** to 1.218 and 1.210 g/cm^3, resp.

Small-Angle-Neutron-Scattering (SANS) Measurements. Instrument *V4* (*Hahn-Meitner-Institut*, Berlin). Measurements were performed at 25° with nearly sat. solns. of polymers **2a** and **2b** in (D_6)DMSO and in 0.1M NaOD/D_2O. For the experiments, a neutron wavelength of 6 Å with a full width at half maximum of 11% was selected, and sample-to-detector distances of 1, 4, and 12 m were employed, which allowed to cover a q range of 0.025–4 nm^{-1}. The solns. were contained in *Hellma* quartz cuvettes with a pathway of 2 mm. The data were recorded by means of a two-dimensional gas detector with 128 × 128 pixels of 0.5 cm size. Data reduction was performed with the 2D data and BerSANS following a regular procedure to account for the electronic noise (measured with cadmium), the transmission and the thickness of the sample, the detector efficiency (determined with the scattering of a H_2O sample of 1 mm thickness), and removing the contribution from the container and the background [35]. An absolute scale was obtained with H_2O as a secondary standard. All corrected data were isotropic and were consequently radial-averaged. Data accumulated at different configurations were finally merged to give the final spectra.

Transmission-Electron-Microscopy (TEM) Measurements. Carbon-coated copper grid (200 mesh; *Science Services*, München, Germany) and *EM922O* mega EFT (energy-filtered transmission) electron microscope (*Zeiss*, Jena); accelerating voltage 200 kV with a beam current of *ca.* 1 μA. A drop (*ca.* 2 μl) of the sample was put on the hydrophilized carbon-coated copper grid. The sample was allowed to adsorb to the activated carbon film for *ca.* 30 s. Subsequently, most of the liquid was removed with blotting paper leaving a thin film stretched on the carbon film which was then air-dried for several minutes. The specimen was inserted into the sample holder and transferred to the transmission-electron microscope.

REFERENCES

[1] a) G. Heller, *Zeitschr. Farben- und Textilchem.* **1903**, *2*, 329 (*Chem. Zentralbl. II* **1903**, 835); b) J. Moir, *Proc. Chem. Soc., London* **1902**, *18*, 194; c) A. Reissert, *Ber. Dtsch. Chem. Ges.* **1914**, *47*, 672.

[2] *Farbwerke* vorm. *Meister, Lucius & Bruening*, DRP 168301, 1905 (*Chem. Zentralbl. I* **1906**, 1204); *Chemische Fabriken* vorm. *Weiler-ter Meer*, DRP 300094, 1916 (*Chem. Zentralbl. II* **1921**, 937).

[3] H. Staudinger, 'Die hochmolekularen organischen Verbindungen', Springer-Verlag, Berlin, 1932.

[4] a) S. J. Holt, *Proc. R. Soc. London, Ser. B* **1954**, *142*, 160; b) A. A. Berlin, A. N. Zelenetskii, B. A. Batik'yan, A. V. Volokhina, G. I. Kudryavtsey, *Khim. Volokna* **1971**, *6*, 19 (CAN 76: 114585, AN 1972: 114585).

[5] a) H. C. Bach, *Polym. Prepr.* **1968**, *9*, 1679; b) E. Ziegler, T. Kappe, H. G. Foraita, L. F. Werner, *Monatsh. Chem.* **1970**, *101*, 923; c) A. A. Berlin, B. I. Ligon'kii, A. N. Zelenetskii, *Izv. Akad. Nauk SSSR, Ser. Khim* **1967**, 225 (CAN 66: 96197; AN 1967: 96197); d) A. A. Berlin, B. I. Liogon'kii, A. N Zelenetskii, *Vysokomol. Soedin., Ser. A* **1968**, *10*, 2076 (CAN 70: 38872; AN 1969: 38872); e) A. A.

Berlin, B. I. Ligon'kii, A. N. Zelenetskii, *Vysokomol. Soedin., Ser. A* **1968**, *10*, 2089 (CAN 70: 12046; AN 1969: 12046); f) A. N. Zelenetskii, L. S. Lyubchenko, M. Y. Kushnerev, A. A. Berlin, *Zh. Struct. Khim.* **1972**, *13*, 50 (CAN 76: 154265; AN 1972: 154265).

[6] a) H. Tanaka, K. Tokuyama, T. Sato, T. Ota, *Chem. Lett.* **1990**, 1813; b) H. Tanaka, *Macromol. Symp.* **1994**, *84*, 137 (CAN 122: 188699; AN 1995: 38415); c) H. Tanaka, T. Sato, C. Ota, JP 04008731, 1992 (CAN 116: 256300; AN 1992: 256300).

[7] T. Yamamoto, K. Kizu, *J. Phys. Chem.* **1995**, *99*, 8.

[8] H. Tanaka, K. Mitsufuji, S. Suematsu, K. Machida, K. Tamamitsu, H. Uchi, JP 084786, 2008 (CAN 148: 452910; AN 2008: 441394).

[9] M. Harada, Y. Abe, F. Kubota, Y. Ohta, WO 069610, 2007 (CAN 147: 96954; AN 2007: 670564); Y. Abe, F. Kubota, Y. Ohta, WO 069611, 2007 (CAN 147: 96600; AN 2007: 670471); Y. Abe, F. Kubota, N. Watanabe, Y. Kidoka, M. Harada, JP 127321, 2008 (CAN 149: 32086; AN 2008: 666518); Y. Kidoka, Y. Abe, N. Watanabe, F. Kubota, M. Harada, JP 056815, 2008 (CAN 148: 332541; AN 2008: 315847); Y. Abe, Y. Kidooka, N. Watanabe, F. Kubota, M. Harada, JP 056814, 2008 (CAN 148: 332540; AN 2008: 315846); N. Watanabe, Y. Abe, Y. Kidooka, F. Kubota, M. Harada, JP 056818, 2008 (CAN 148: 332545; AN 2008: 316951).

[10] J. T. Guthrie, *Rev. Prog. Color.* **1990**, *20*, 40; D. J. Dawson, *Aldrichimica Acta* **1981**, *14*, 23; R. W. Moncrieff, *Int. Dyer, Textile Printer, Bleacher Finisher* **1973**, *150*, 27 (CAN 79: 116267; AN 1973: 516267).

[11] a) H. Zollinger, 'Color Chemistry. Syntheses, Properties, and Applications of Organic Dyes and Pigments', 3rd edn., Verlag Helvetica Chimica Acta, Zürich, Wiley-VCH, Weinheim, 2003; b) P. Suesse, M. Steins, V. Kupcik, *Z. Kristallogr.* **1988**, *184*, 269.

[12] a) S. Ganapathy, R. G. Zimmermann, R. G. Weiss, *J. Org. Chem.* **1986**, *51*, 2529; b) Y. Omote, A. Tomotake, H. Aoyama, T. Nishio, C. Kashima, *Bull. Chem. Soc. Jpn.* **1984**, *57*, 470; c) Y. Omote, K. Fujiki, H. Awano, I. Kubota, T. Nishio, H. Aoyama, *Bull. Chem. Soc. Jpn.* **1981**, *54*, 627.

[13] B. Capon, F. C. Kwock, *J. Am. Chem. Soc.* **1989**, *111*, 5346.

[14] J. D. Thoburn, W. Luettke, C. Benedict, H.-H. Limbach, *J. Am. Chem. Soc.* **1996**, *118*, 12459; H. Sieghold, W. Luettke, *Angew. Chem.* **1975**, *87*, 63.

[15] J. Blanc, D. L. Ross, *J. Phys. Chem.* **1968**, *72*, 2817.

[16] B. D. Smith, M.-F. Paugam, K. J. Haller, *J. Chem. Soc., Perkin Trans.* **1993**, *2*, 165.

[17] P. W. Sadler, R. L. Warren, *J. Am. Chem. Soc.* **1956**, *78*, 1251; H. C. F. Su, K. C. Tsou, *J. Am. Chem. Soc.* **1960**, *82*, 1187.

[18] G. A. Russell, G. Kaup, *J. Am. Chem. Soc.* **1969**, *91*, 3852.

[19] a) D. Vorlaender, J. von Pfeiffer, *Ber. Dtsch. Chem. Ges.* **1919**, *52*, 325; b) P. Friedlaender, E. Schwenk, *Ber. Dtsch. Chem. Ges.* **1910**, *43*, 971.

[20] a) M. Kurihara, N. Yoda, *Bull. Chem. Soc. Jpn.* **1967**, *40*, 2429; b) *BASF*, DRP 43524, 1887 (in *Ber. Dtsch. Chem. Ges.* **1888**, *R 21*, 492).

[21] K. Heumann, *Ber. Dtsch. Chem. Ges.* **1890**, *23*, 3431; T. Wieland, W. Sucrow, 'Gattermann, Wieland, Die Praxis des organischen Chemikers', 43rd edn., Walter de Gruyter, Berlin, 1982, p. 651.

[22] G. Voss, W. Schramm, *Helv. Chim. Acta* **2000**, *83*, 2884.

[23] T. Hosoe, K. Nozawa, N. Kawahara, K. Fukushima, K. Nishimura, M. Miyaji, K. Kawai, *Mycopathologia* **1999**, *146*, 9.

[24] H. F. Braun, G. Voss, unpublished results.

[25] G. Voss, M. Gradzielski, J. Heinze, H. Reinke, C. Unverzagt, *Helv. Chim. Acta* **2003**, *86*, 1982.

[26] 'NMR of Macromolecules. A Practical Approach', Ed. G. C. K. Roberts, Oxford University Press, Oxford – New York – Tokyo, 1995, p. 7.

[27] C. Miliani, A. Romani, G. Favaro, *Spectrochim. Acta, Part A* **1998**, *54*, 581.

[28] K. Yamada, T. Konakahara, H. Iida, *Chiba Daigau Kogakubu Kenkyu Hokoku* **1970**, *21*, 157 (*Chem. Abstr.* **1972**, *77*, 36359).

[29] H. von Eller, *Acta Crystallogr.* **1952**, *5*, 142.

[30] A. Guinier, G. Fournet, 'Small-Angle Scattering of X-rays', Wiley, New York, 1955.

[31] J. S. Pedersen, *Adv. Colloid Interface Sci.* **1997**, *70*, 171.

[32] J. S. Pedersen, in 'Neutrons, X-rays and Light: Scattering Methods Applied to Soft Condensed Matter', Eds. P. Lindner and T. Zemb, Elsevier, Amsterdam, 2002, p. 391; T. M. Weiss, T. Narayanan, M. Gradzielski, *Langmuir* **2008**, *24*, 3759.
[33] K. Lu, J. Jacob, P. Thiyagarajan, V. P. Conticello, D. G. Lynn, *J. Am. Chem. Soc.* **2003**, *125*, 6391; P. Thiyagarajan, J. J. Dong, R. P. Apkarian, D. G. Lynn, *Bioorg. Med. Chem.* **2005**, *13*, 5213.
[34] ' Handbook of Chemistry and Physics', 56th edn., CRC Press, 1975, D-261.
[35] U. Keiderling, *Appl. Phys. A* **2002**, *74*, 1455.

Received April 3, 2009